PERGAMON

International Journal of Heat and Mass Transfer 45 (2002) 4289–4303

International Journal of HEAT and MASS TRANSFER

www.elsevier.com/locate/ijhmt

Frost formation and frost crystal growth on a cold plate in atmospheric air flow

Chin-Hsiang Cheng *, Chiuan-Che Shiu

Department of Mechanical Engineering, Tatung University, 40 Chungshan N. Road, Sec. 3 Taipei, 10451 Taiwan, ROC

Received 12 September 2001; received in revised form 26 March 2002

Abstract

The present study is concerned with the spatial variation of the frost thickness as well as the pattern of the frost crystals formed on a cold plate in atmospheric air. Experimental results regarding the two-dimensional variation of the frost thickness at the leading edge and observation on the growth of the frost crystals on the frost formation are provided. A microscopic image system is used to observe the structure of the frost layer. The environmental variables considered in this study include the velocity, temperature, and relative humidity of the air (V, T_a, and ϕ), as well as the surface temperature of the cold plate (T_w), which is varied by adjusting the cooling refrigerant temperature (T_{ref}). The ranges of the physical variables considered in this study are $2 \leqslant V \leqslant 8$ m/s, $18 \leqslant T_a \leqslant 30$ °C, $40\% \leqslant \phi \leqslant 70\%$, $-18 \leqslant T_{ref}$ (and T_w) $\leqslant 0$ °C.

Keywords: Frost thickness; Frost crystal; Cold plate; Image system

1. Introduction

When atmospheric air flows over a surface of which the temperature is below the dew point temperature of the air, the water vapor in the air will condense on the surface. Furthermore, when the surface temperature is lower than the freezing point of the liquid condensate, frost or ice will form on the cold surface. During these condensation or solidification process, latent heat of vaporization or fusion is released by the water vapor in the atmospheric air, and mass of water continues to accumulate on the cold surface as a form of liquid condensate or frost crystal. These phase change phenomena are commonly encountered on surfaces of thermal devices and relevant to a number of engineering problems related to low-temperature heat exchanger, air conditioning systems, frozen food industry, and so on. Therefore, these phenomena have received great attention in recent years. As reported by Emery and Siegel [1], a 50–75% decrease in heat transfer and a substantial increase in pressure drop are caused by frost formation on a compact heat exchanger. Therefore, owing to the subtle influence of frost formation on thermal and flow characteristics of the heat exchangers, the frost formation problems are worthy of further investigation.

Based on the experimental observations provided by Hayashi et al. [2], the frost formation process may be subdivided into three periods: (a) crystal growth period, (b) frost layer growth period, and (c) frost layer fully growth period. Meng et al. [3] treated the frost layer as a porous medium and presented a physical model for predicting the growth rate of frost formation. Brian et al. [4], Jones and Parker [5], Sami and Duong [6], and Sherif et al. [7] assumed that the amount of water vapor of the atmospheric air moving toward the frost layer is approximately divided into two parts. One part of water vapor enters the existing frost layer for solidification and increases the density throughout the frost layer. The other part rests on the surface of frost layer, and the solidification of this part of water vapor increases the frost thickness. Therefore, both the density and the thickness of the frost layer increase with time. However,

* Corresponding author. Tel.: +886-2-25925252x3410; fax: +886-2-25997142.

E-mail address: cheng@ttu.edu.tw (C.-H. Cheng).

0017-9310/02/$ - see front matter
PII: S0017-9310(02)00134-5

Nomenclature

t	time (min)
T_a	air temperature (°C)
T_i	inlet temperature of cooling refrigerant (°C)
T_o	exit temperature of cooling refrigerant (°C)
T_{ref}	cooling refrigerant temperature (°C)
T_w	cold plate temperature (°C)
V	air velocity (m/s)
X, Y, Z	Cartesian coordinates (mm)
Y_s	frost thickness (mm)

Greek symbol

ϕ	relative humidity (%)

the variation of the mass fractions of these two parts of water vapor is still unknown. Tao et al. [8] studied the initial growth of frost on a flat plate subjected to a forced convective air flow and observed a two-stage frost formation process, for the flat plate suddenly cooled to a temperature below the freezing point of water. The first stage corresponds to the liquid condensation taking place on the flat plate, and in the second stage, the ice crystals start growing in an ice-column fashion that can be approximated by a one-dimensional ice-column model. In addition, two possible frost growth patterns, monotonic growth and cyclic growth, were seen by Östin and Andersson [9]. The cyclic frost growth is attributed to the frost melting on the frost surface that produces larger amount of liquid penetrating into the frost layer and thus results in abrupt internal solidification. When the melting and the internal solidification proceed, the internal thermal resistance is gradually reduced. Eventually the frost surface temperature drops to a value below the freezing point again and then the frost thickness starts to grow. The initiation and the growth of the frost formation on a flat plate were further investigated by Şahin [10]. He found that the diffusion of water vapor through the void portions of the frost layer during the crystal growth period is insignificant except for the cases with very low plate temperature.

On the other hand, the dependence of the frost growth pattern on the environmental variables and surface conditions has been studied extensively. However, since the frost formation process is really involved, even in the idealized cases of a humid air over a flat cold plate, a detailed physical picture for the frost formation is still not clear. For example, data provided by the previous studies [10–13] concerning the air velocity effects on frost formation are not in agreement. O'Neal and Tree [11,12] observed that the frost growth rate increases with air velocity only as Reynolds number is less than 15 900. At a Reynolds number higher than this value, the frost growth shows no dependence on the Reynolds number. Furthermore, it is noted that even for the air temperature effects, inconsistencies between the existing reports are also found. Şahin [10] and Lüer and Beer [13] observed a thinner and denser frost layer at a higher air temperature. However, O'Neal and Tree [11] found no appreciable difference in the frost thickness measurements in a three-hour duration.

In addition to the experimental works, a number of theoretical models for predicting the growth rate of the frost layer have also been presented. These theoretical models are developed based on the conservation of mass and conservation of energy principles and normally consist of a set of ordinary or partial differential equations plus several required property relations. The models proposed by Meng et al. [3], Jones and Parker [5], Sami and Duong [6], Sherif et al. [7], and Padki et al. [14], are several examples dealing with the ordinary differential equations. Recently, the models due to Jones and Parker [5] and Sherif et al. [7] have been modified by Cheng and Cheng [15], and a simple but efficient model has been presented. The theoretical model of Cheng and Cheng [15] is verified by Wu [16] with experimental data. Transient variation of the local frost thickness in the downstream region is measured by Wu [16], and it is found that the model of Cheng and Cheng [15] is particularly valid for the frost layer growth period.

Based on the aforementioned studies, it may be noted that even though the frost formation on a cold plate has been investigated extensively, the existing information regarding the observations of early-stage frost formation on the cold plate is still insufficient, especially for the crystal growth. Furthermore, the attention of most of these existing studies was focused on the measurement for a local frost thickness at a fixed position on the cold plate, the two-dimensional variation of the frost thickness in the streamwise direction has not been well discussed. Therefore, the information for the spatial variation of the frost layer thickness is still lacking.

In these circumstances, the present study is aimed to investigate the two-dimensional variation of the frost thickness on a cold plate. The emphasis is placed at the leading edge of the cold plate where maximum frost thickness is usually observed. Effects of velocity, temperature, and relative humidity of air (V, T_a, and ϕ) are examined, and the surface temperature of the cold plate (T_w) is also varied by adjusting the temperature and the mass flow rate of the cooling refrigerant (T_{ref}). The ranges of the physical variables considered in this study are: $2 \leqslant V \leqslant 8$ m/s, $18 \leqslant T_a \leqslant 30$ °C, $40\% \leqslant \phi \leqslant 70\%$,

$-18 \leqslant T_{ref}$ (and T_w) $\leqslant 0$ °C. Observations on the frost crystal growth are performed by using a microscopic image system. The transient variation of the crystal pattern has been recorded so as to investigate the dependence of crystal structures on the physical conditions.

2. Experimental apparatus and procedures

2.1. Experiment apparatus

The layout of the entire experiment system is shown in Fig. 1. The experiments were performed in the test section of a suction-type open-loop wind tunnel. The wind tunnel has a length of 5.5 m and consists of a contraction section, a honeycomb section, the test section, and a fan section. The test section of the wind tunnel, which has a 300 mm × 300 mm cross section and a length of 1.6 m, is made with plexiglas plate of 10 mm thickness so that the frost layer can be clearly observed by the microscopic image system. The entrance contraction and the honeycomb sections are placed in front of the test section. The honeycomb section contains about 2000 subchannels, each with a length-to-diameter ratio of 34. The air velocity may be varied in the range of 0 to 40 m/s by means of a frequency regulator connected to the fan motor. A chiller (Model No. B403-D made by FIRSTEK SCIENTIFIC) is used to provided a circulation of the low-temperature refrigerant for cooling purpose. The refrigerant, methanol, can be cooled down to lowest −20 °C in the chiller and then is introduced into a cold plate and cooling unit assembly. The cold plate is made of copper (C1220) with surface roughness of 0.57 μm. The length and the width of the cold plate are both fixed at 55 mm, and the thickness of it is 8 mm. The cold plate is mounted on a cooling unit, through which the low-temperature methanol is circulated. The cooling unit is made of Plexiglas whose thermal conductivity is sufficiently low so as to reduce the heat transfer to the cooling unit from the surrounding. The cold plate is aligned with the bottom surface of the test

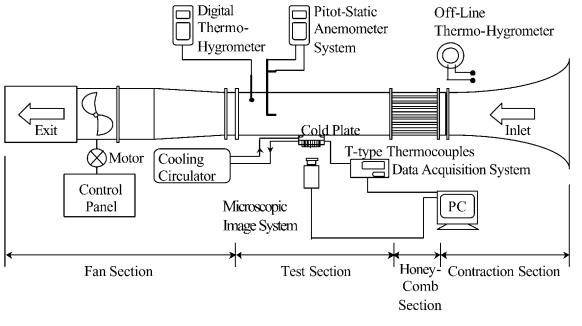

Fig. 1. Experiment system.

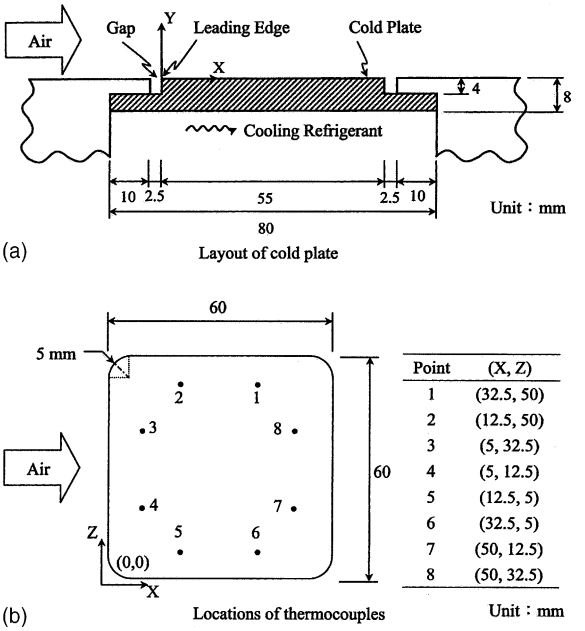

Point	(X, Z)
1	(32.5, 50)
2	(12.5, 50)
3	(5, 32.5)
4	(5, 12.5)
5	(12.5, 5)
6	(32.5, 5)
7	(50, 12.5)
8	(50, 32.5)

Fig. 2. Cold plate and cooling unit assembly: (a) layout of cold plate, (b) locations of thermocouples.

section, and its lateral faces are insulated by a bakelite layer. By adjusting the mass flow rate of methanol, the temperature of the cold plate may be varied in the range of −18 to 0 °C for different experiments. The layout of the cold plate and the location of the installed thermocouples are plotted in Fig. 2(a) and (b), respectively.

The microscopic image system consists of a CCD camera (Model No. IK-624F, TOSHIBA), a zoom/enlarging lens unit (Model No. 29-95-92/29-90-74, OPTEM), and a luminescence house/annular illuminator unit (Model No. 29-60-02/29-60-31, OPTEM). The CCD camera and the zoom/enlarging lens unit, which is at maximum of 158× magnification, are mounted by the side of the test section for taking the photographs of the frost formation at adjustable time interval. The annular illuminator unit provides luminescence light for observation but does not emit appreciable thermal radiation to destroy to the frost layer. A personal computer (Pentium III 733MHz) equipped with a color PCI frame grabber, receives the image data taken at every 5 s by the microscopic image system. The images are analyzed with an image processor (MATROX software, Inspector version 2.1). A software-based microscale having 80–200 pixels in 1 mm is developed by the image processor at. A 1-mm objective microruler manufactured by OLYMPUS is used as a standard ruler for calibrating themicroscale at a resolution of 1/80 mm per pixel in both X- and Y-directions. Therefore, as the number of pixel scales occupied by the area of the frost layer is

determined with the image processor, the thickness of the frost layer can then be calculated.

The temperature of the cold plate is measured by eight T-type thermocouples installed at eight different locations uniformly distributed in the cold plate, as already shown in Fig. 2(b). All the thermocouple probes are placed at the same level of 3 mm beneath the surface of the cold plate. Temperature data are recorded by a data acquisition system (Model No. NetDAQ 2640A, FLUKE). The thermocouple wires are inserted into the cold plate from its lateral faces and connected to the data acquisition system from under the bottom face of the test section to eliminate possible disturbance to the

Table 1
Uncertainty analysis for measured variables

Variable	Tyical value (x)	Uncertainty (δx)
V (m/s)	2.0–8.0	0.4
ϕ (%)	40–70	3
T_a (°C)	18–30	0.1
T_{ref} (°C)	−18 to 0	0.1
T_w (°C)	−18 to 0	1.0
T_i (°C)	−20 to −10	0.1
T_o (°C)	−20 to −10	0.1
X (mm)	−2.5 to 5.0	0.03
Y_s (mm)	0–4	0.03

All values estimated with 95% confidence.

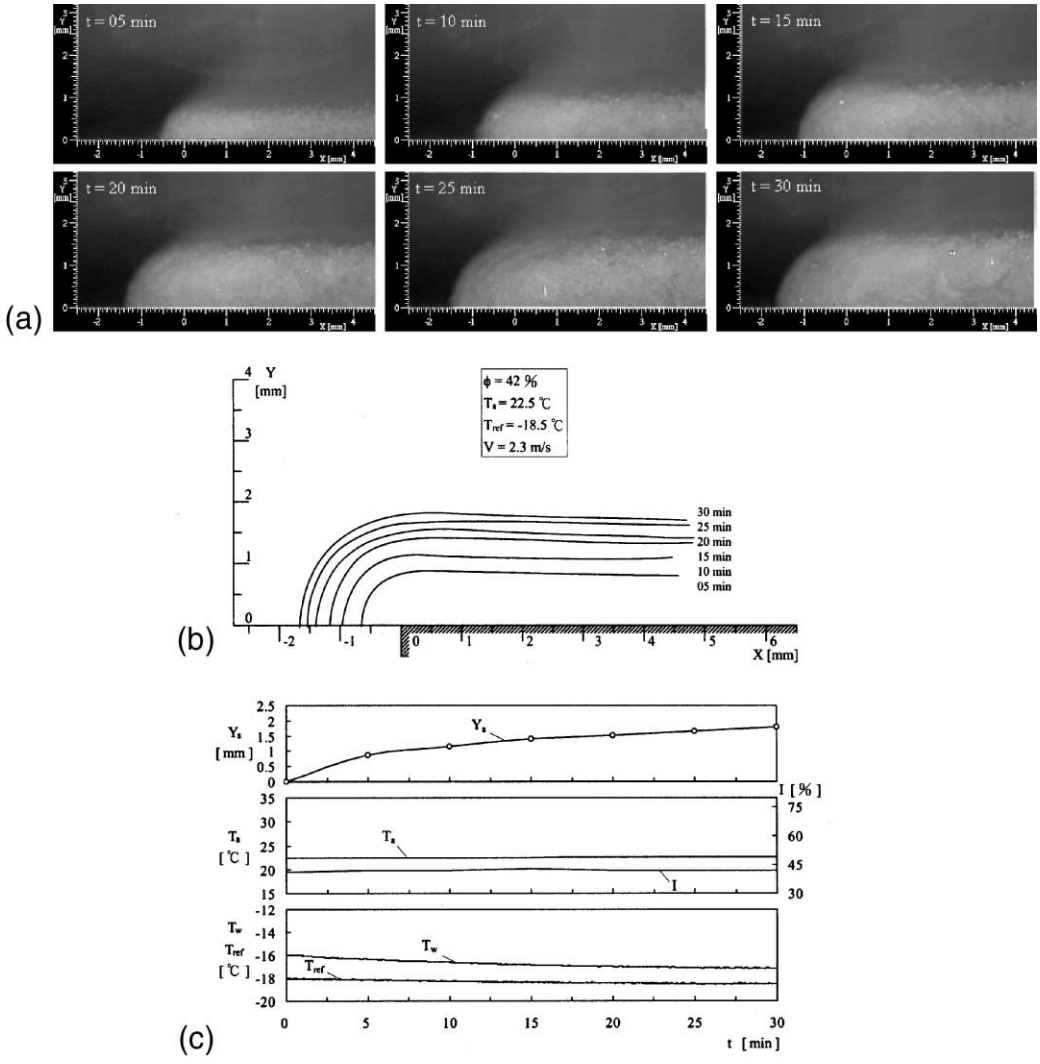

Fig. 3. Growth of the frost layer adjacent to the leading edge for $\phi = 42\%$, $T_a = 22.5$ °C, $T_{ref} = -18.5$ °C, and $V = 2.3$ m/s: (a) photographs of the frost layer, (b) outlines of the frost layer, (c) environmental conditions and the frost thickness at $X = 0$.

air flow. The uniformity of the temperature distribution on the cold plate surface has been observed based on the temperature data measured by the eight thermocouples. In addition, two T-type thermocouples are mounted at the inlet and the exit of the cooling unit to measure the inlet and exit temperatures of methanol (T_i and T_o). The temperature data recorded by the data acquisition system are finally transferred to the personal computer for further analysis and printing out.

A thermo-hygrometer (Model No. HOBO Pro H08-032-08) is installed to monitor the environmental conditions, including temperature and relative humidity of the ambient air. The thermo-hygrometer can be used for long-term measurement in the off-line mode. Meanwhile, in this study, the temperature (T_a) and relative humidity (ϕ) of the incoming air are measured by using another thermo-hygrometer (Model No. THG338, DIGITAL) installed in the test section. The air temperature measured by the meter is compared with those measured by a T-type thermocouple to ensure the accuracy of the measurement. The accuracy of the probe is 3% for relative humidity and ± 0.1 °C for temperature at full range.

A pitot-static anemometer system consisting of a pitot-static probe, connecting pipe for transmission of the differential pressures, and a differential pressure transducer is used for velocity measurement. The pitot tube (1/8″ diameter, Dwayer) is mounted in the downstream area of the test section to reduce possible interference with the air flow over the cold plate. The differential

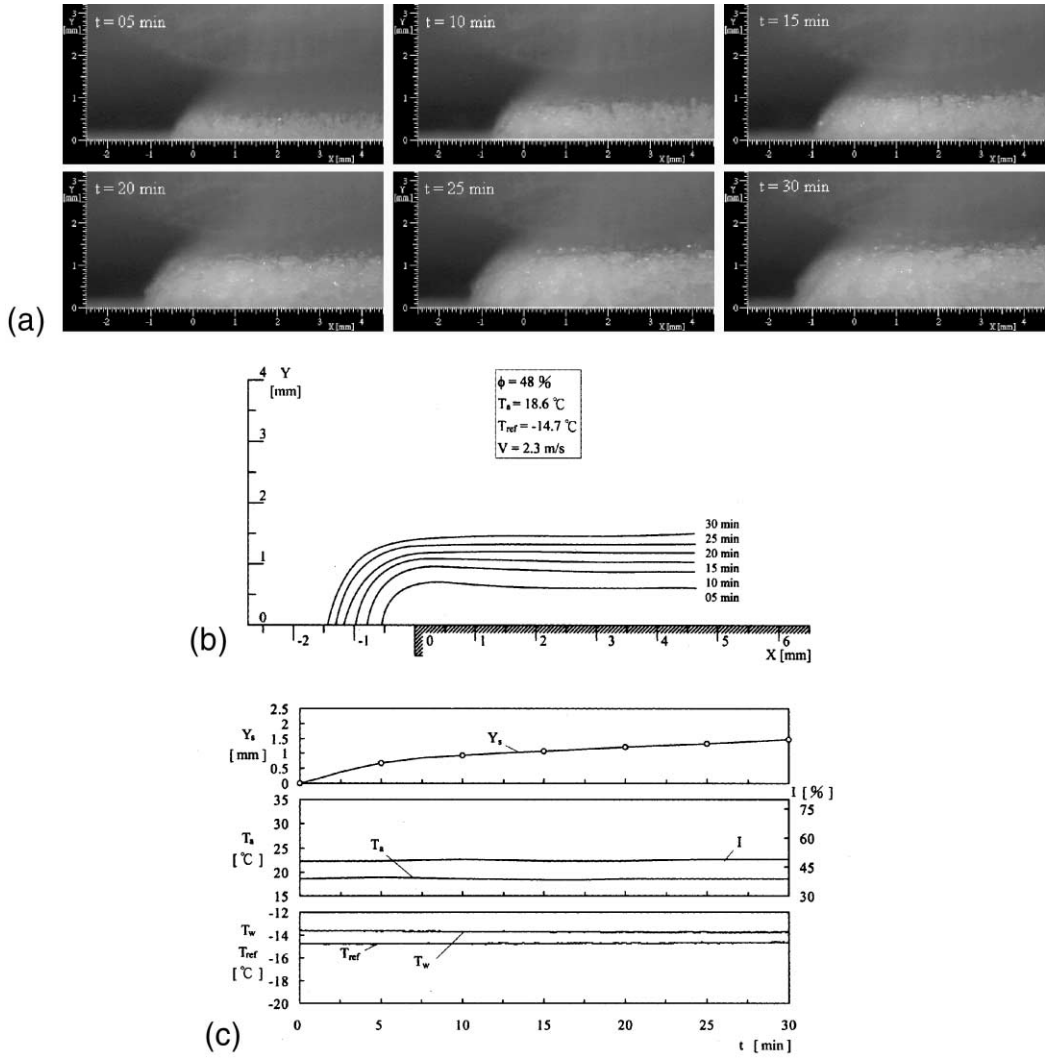

Fig. 4. Growth of the frost layer adjacent to the leading edge for $\phi = 48\%$, $T_a = 18.6$ °C, $T_{ref} = -14.7$ °C, and $V = 2.3$ m/s: (a) photographs of the frost layer, (b) outlines of the frost layer, (c) environmental conditions and the frost thickness at $X = 0$.

pressure signal developed at the pitot tube is transmitted to the differential pressure transducer, and then this signal is converted to air velocity by performing a mathematical conversion. The resolution and accuracy of the differential pressure transducer used in this study are 0.01 mmH_2O and $\pm 0.2\%$ full range, respectively. In this study, the air velocity is varied between 2 and 8 m/s.

2.2. Measurement procedures

The uncertainty resulting from the cold plate surface contamination should be minimized. Therefore, the surface is cleaned and covered with a sheet of plastic film before test. The frequency regular and the exit valve of the wind tunnel are adjusted to set the desired air velocity. The methanol is cooled to a sufficiently low temperature (−18 to 0 °C) and circulated by using the chiller prior to the test. The cold plate is maintained at a desired temperature by the circulation of methanol, and its temperature is varied between −18 and 0 °C in this study. The personal computer receives the temperature data from the thermocouples as well as the images from the microscopic image system. The photographs recording the frost formation are taken at a sampling rate specified beforehand, and a normal experiment duration is 30 min. Typically, for each test 360 images in 30 min are recorded by the computer for further analysis such that the rapid changes in the frost growth process would not be ignored. The spatial variation of the frost thickness at the leading edge of the cold plate is measured by the microscale at different time instants. Meanwhile, the frost crystals are observed by using the microscopic image

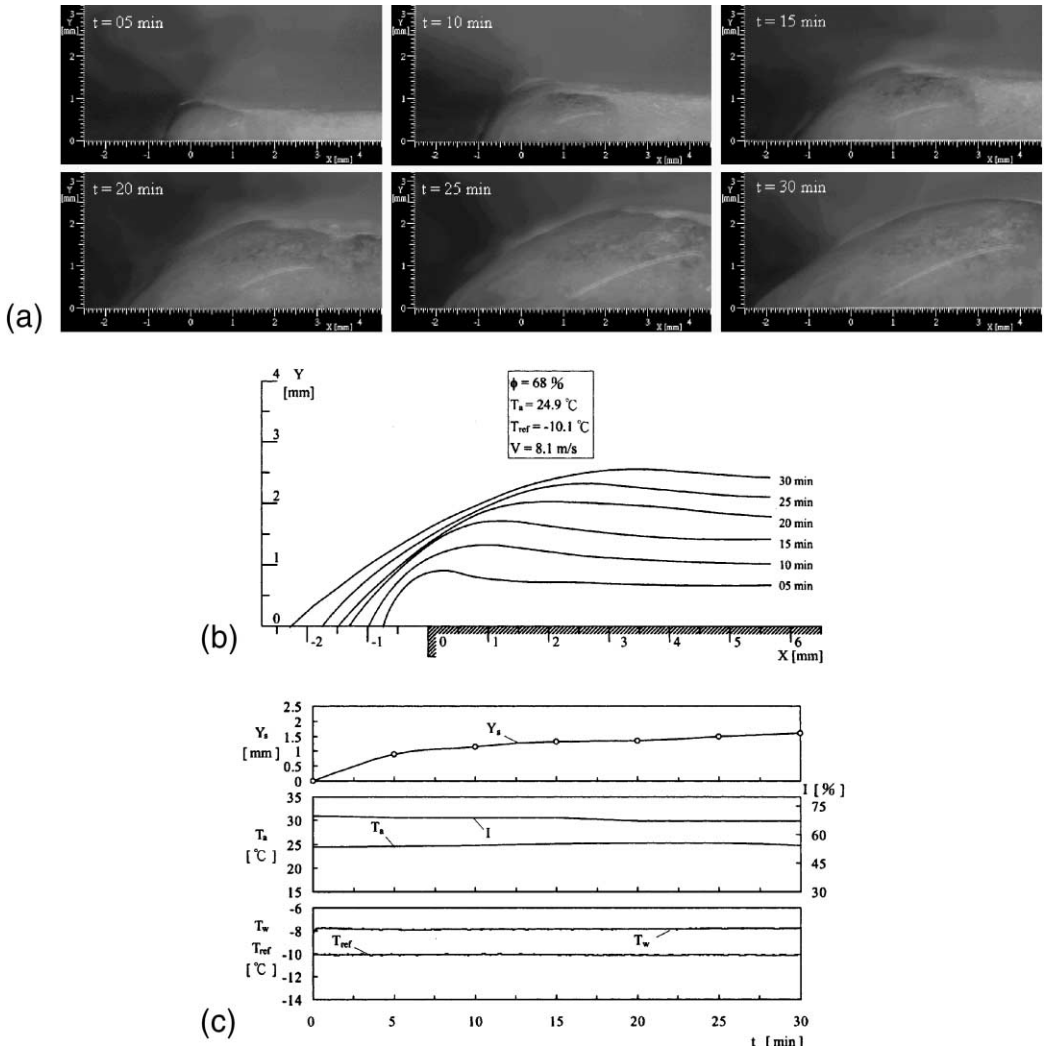

Fig. 5. Growth of the frost layer adjacent to the leading edge for $\phi = 68\%$, $T_a = 24.9$ °C, $T_{ref} = -10.1$ °C, and $V = 8.1$ m/s: (a) photographs of the frost layer, (b) outlines of the frost layer, (c) environmental conditions and the frost thickness at $X = 0$.

system. During the experiment process, the temperature and the relative humidity of the incoming air flow are continuously recorded by the thermo-hygrometer, and the air velocity is measured and monitored by the anemometer. The conditions of the ambient air are always monitored by the off-line thermo-hygrometer.

In the experiment, the uncertainty may be caused by a number of sources. For example, the uncertainty may come from the accuracy of the instrument, the calibration errors, the uncertainties of environmental conditions, and so on. In this study, the uncertainty interval for each measured variable is evaluated with a 95% confidence based on the concepts proposed by Kline and McClintock [17] and Moffat [18]. These concepts were adopted by Wu [16] and Cheng et al. [19] in estimating the uncertainties for the same experiment system, and description of the evaluation method is available in Refs. [16,19]. The results of uncertainty analysis for the physical parameters measured in this study are provided in Table 1. It is observed in this table that the relative humidity of air contributes the largest uncertainty, 3%, in the experiment.

3. Results and discussion

3.1. Two-dimensional variation of frost thickness

The scope of the microscopic image system is focused on the area of −2.5 to 5.0 mm from the leading edge. Time interval of sampling is 5 s in the experiment. The image of the frost layer is taken by the microscopic image system, and then the variation of the frost thickness is measured by using the image processor.

Fig. 3 shows the growth of frost layer adjacent to the leading edge. For the case at $\phi = 42\%$, $T_a = 22.5$ °C, $T_{ref} = -18.5$ °C, and $V = 2.3$ m/s, the snapshots of the frost layer are observed in Fig. 3. In this study, one image is recorded per 5 s; however, only the photographs for every five minutes are displayed in this figure

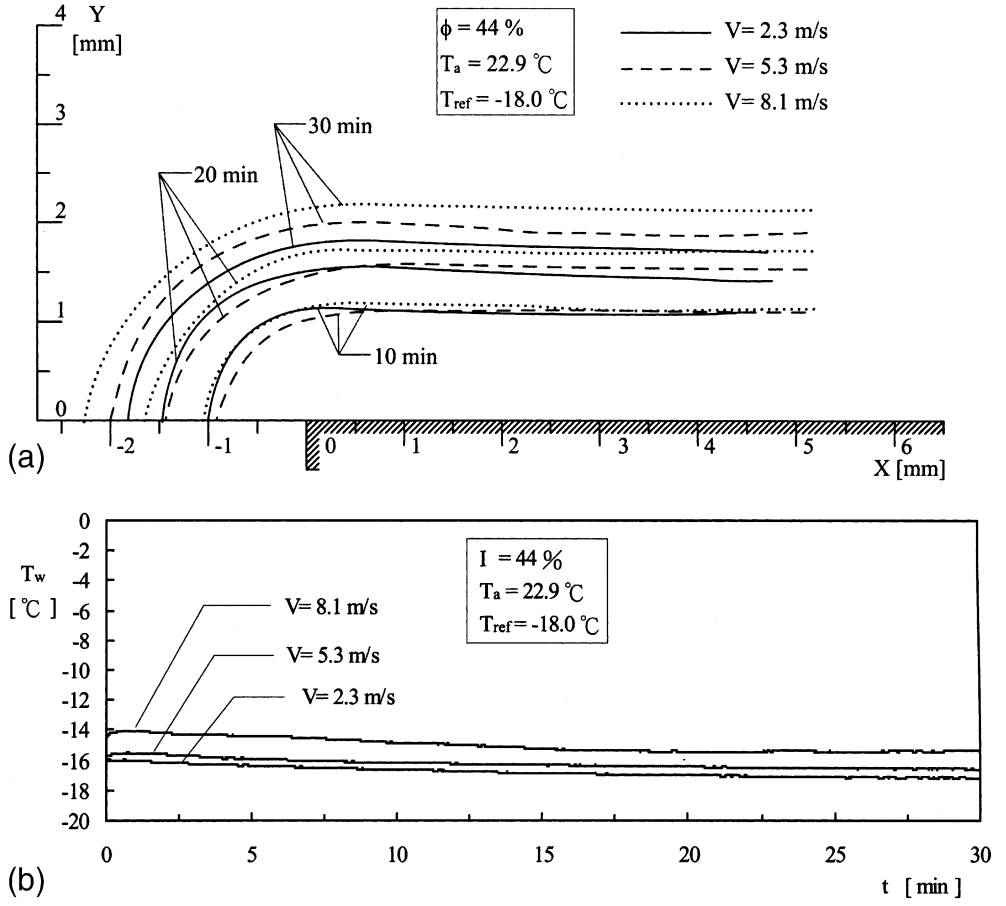

Fig. 6. Effects of air velocity on growth of frost layer adjacent to the leading edge at $\phi = 44\%$, $T_a = 22.9$ °C, and $T_{ref} = -18.0$ °C: (a) outlines of the frost layer, (b) histories of cold plate temperature at various air velocities.

to save space. At the beginning of the frost formation process, the cold plate is covered by small, isolated crystal columns growing in the direction normal to the cold plate. At $t = 5$ min, it is observed that a thin frost layer of thickness approximately 0.8 mm is formed. Then, the thickness and the density of the frost layer both increase with time. Note that at the leading edge of the cold plate, the frost crystals grow not only in the direction normal to the cold plate, but also in the direction opposite to the direction of air stream. As a matter of fact, the frost crystals grow in radial direction at the leading edge to form a 'round head'. The round head of the frost layer at the leading edge is streamlined by the air flow so that the profile of the round head of the frost layer is rather smooth. In the area adjacent to the leading edge, the thickness of the frost layer is definitely a function of the streamwise location. It is found that in the downstream region, the frost crystals grow at approximately the same rate, and a homogeneous frost layer of uniform thickness is seen. History of the one-dimensional frost thickness in the downstream region was measured by Wu [16], and the uniformity in the frost thickness in the downstream region tends to confirm the one-dimensional behavior of the frost layer assumed by Wu [16]. However, at the leading edge of the cold plate, the frost thickness is not uniform any longer but features a two-dimensional smooth profile. The frost layers at various time instants are outlined by means of the image processor and shown in Fig. 3(b). The outlines of the frost layer are portrayed by the image processor based on the intensity of all the pixels of the frost layer images. The variation of the frost layer outline clearly shows the history of the frost layer at the leading edge of the cold plate.

Fig. 3(c) displays the histories of frost thickness at $X = 0$ (Y_s), the relative humidity and temperature of air (ϕ and T_a), and the temperatures of the cold plate and the cooling refrigerant (T_w and T_{ref}). Frost layer at the location of $X = 0$ is brought into focus of the microscopic system, and the frost thickness at the location is

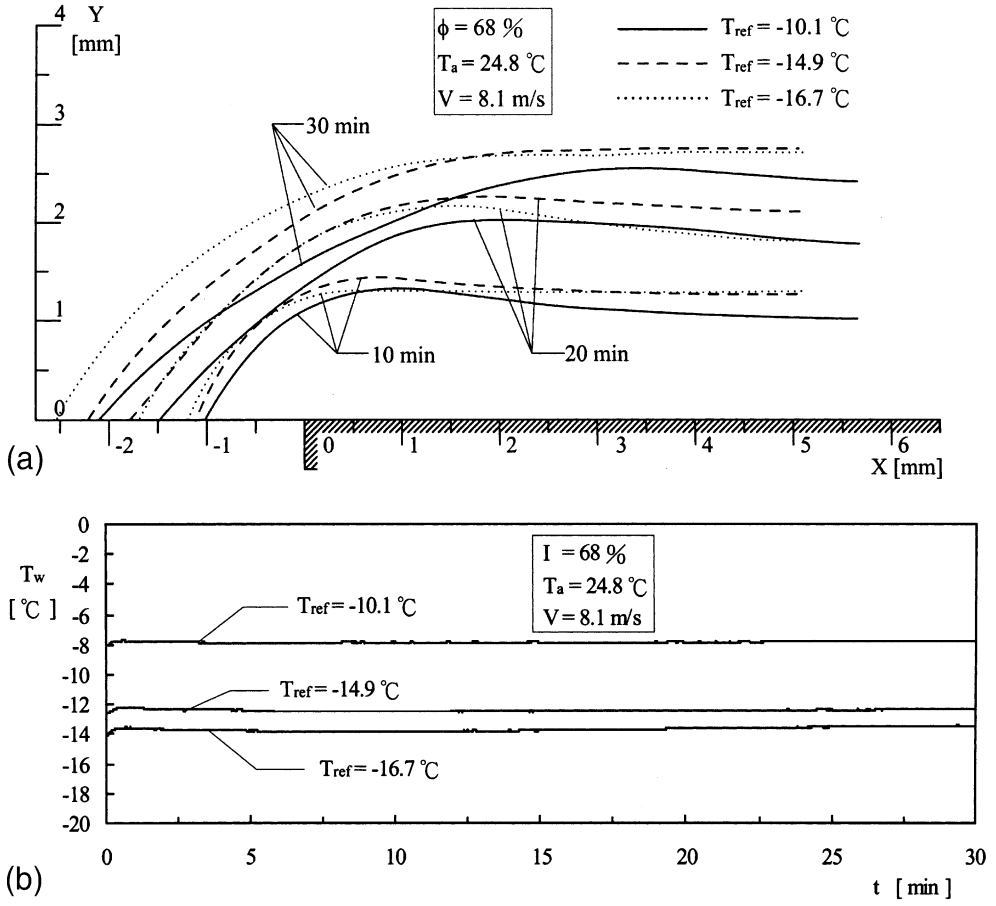

Fig. 7. Effects of cooling refrigerant temperature on growth of frost layer adjacent to the leading edge at $\phi = 68\%$, $T_a = 24.8$ °C, and $V = 8.1$ m/s: (a) outlines of the frost layer, (b) histories of cold plate temperature at various air velocities.

measured. The extent of the frost layer increases with time since new frost crystal columns continue to grow on top of the frost layer, and the density of the frost layer is increased by the formation of crystal branches stemming from the existing crystal columns. This period is referred to as the frost layer growth period. Note that the thickness of the frost layer at $X = 0$ is increased to be 1.89 mm at $t = 30$ min. During the 30-min duration of experiment, the frost layer full growth period is not reached. In addition, based on the histories of T_a, ϕ, and T_{ref} presented in Fig. 3(c), it is observed that T_a, ϕ, and T_{ref} are fixed at constant values with acceptable uncertainties, whereas T_w is found to slightly descend in the 30-min duration. However, the change of T_w is less than 1.3 °C during the experiment. Note that the value of T_w is an average value of the temperatures measured by eight thermocouples installed in the cold plate. The uniformity of the temperature distribution in the cold plate has been observed with a maximum error within 1 °C based on the temperature data measured by the eight thermocouples.

Figs. 4 and 5 show the comparison in the frost layer growth at the leading edge for two limiting cases. The former case considers a relatively dry ($\phi = 48\%$), cold ($T_a = 18.6$ °C), and low-velocity ($V = 2.3$ m/s) air flow over a cold plate at $T_{ref} = -14.7$ °C, and the results are provided in Fig. 4. The latter case considers a relatively humid ($\phi = 68\%$), warm ($T_a = 24.9$ °C), and high-velocity ($V = 8.1$ m/s) air flow over a cold plate at $T_{ref} = -10.1$ °C, and the results are given in Fig. 5. In Fig. 4, the frost layer appears to be dry and has lower density, whereas the frost layer for the case shown in Fig. 5 is always melting and wet and hence, has a high density. These two figures clearly convey the dependence of the frost layer structure on the environmental variables.

A deeper insight into the influence of the environmental variables on the frost layer growth may be gained

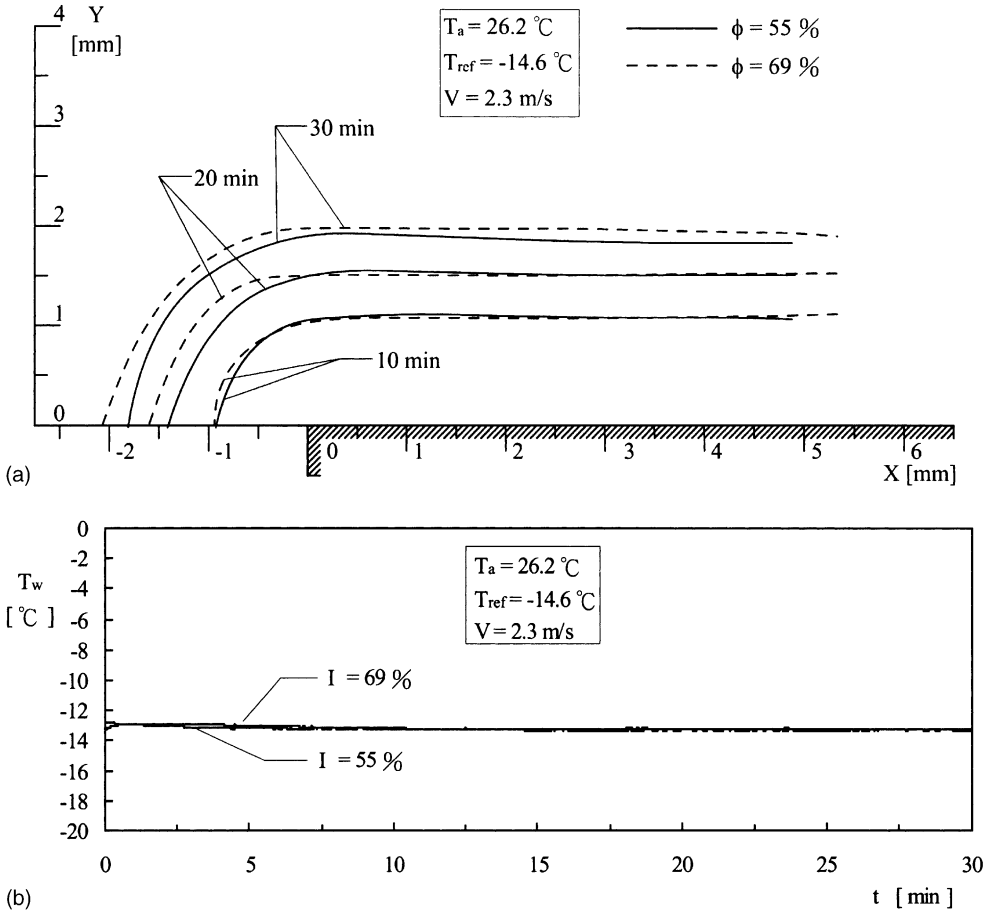

Fig. 8. Effects of relative humidity of air on growth of frost layer adjacent to the leading edge at $T_a = 26.2$ °C, $T_{ref} = -14.6$ °C, and $V = 2.3$ m/s: (a) outlines of the frost layer, (b) histories of cold plate temperature at various air velocities.

from the information displayed in Fig. 6. The attention is now focused on the outlines of the frost layer. Fig. 6 shows the effects of air velocity on the growth of the frost layer adjacent to the leading edge, at $\phi = 44\%$, $T_a = 22.9$ °C, and $T_{ref} = -18.0$ °C. In this figure, the air velocity is assigned to be 2.3, 5.3, or 8.1 m/s. It can be expected that heat and mass transfer to the frost layer may increase with the air velocity and therefore, either the frost density or the frost thickness will be elevated by increasing the air velocity. For those cases in which the frost thickness does not increase significantly with the air velocity, there is always a significant increase in the frost density. In Fig. 6(a), the growth rate of the frost thickness generally increases with the air velocity. On the other hand, a higher air velocity leads to stronger heat convection on the frost surface. A stronger heat convection results in a higher cold plate temperature. The cold plate temperature is increased by approximately 2 °C when the air velocity is elevated from 2.3 to 8.1 m/s, as show in Fig. 6(b). Note that in Fig. 6(b) the temperature of the cooling refrigerant is fixed at −18 °C.

Fig. 7 conveys the effects of cooling refrigerant temperature on the growth of frost layer. In Fig. 7, the case at $\phi = 68\%$, $T_a = 24.8$ °C, and $V = 8.1$ m/s is considered. It is found that the cold plate temperature increases with the cooling refrigerant temperature. The temperature difference between T_w and T_{ref} is about 2–3 °C. However, the cold plate temperatures are nearly kept constant in the experiments. Decreasing the cooling refrigerant temperature from −10.1 to −16.7 °C leads to a significant increase in the thickness as well as a change in the shape profile of the frost layer. A similar tendency for the cold plate surface temperature effect has been found by a number of authors [9,10,13].

Fig. 8 depicts the effects of the relative humidity of air on the growth rate of the frost layer. The data presented in Fig. 8 for the case at $T_a = 26.2$ °C, $T_{ref} = -14.6$ °C, and $V = 2.3$ m/s clearly illustrate that the frost thickness increases with the moisture content of the air. However, it is expected that the cold plate temperature is nearly independent of the relative humidity. In Fig. 8(b), the curves for cold plate temperatures at $\phi = 55\%$ and 69%

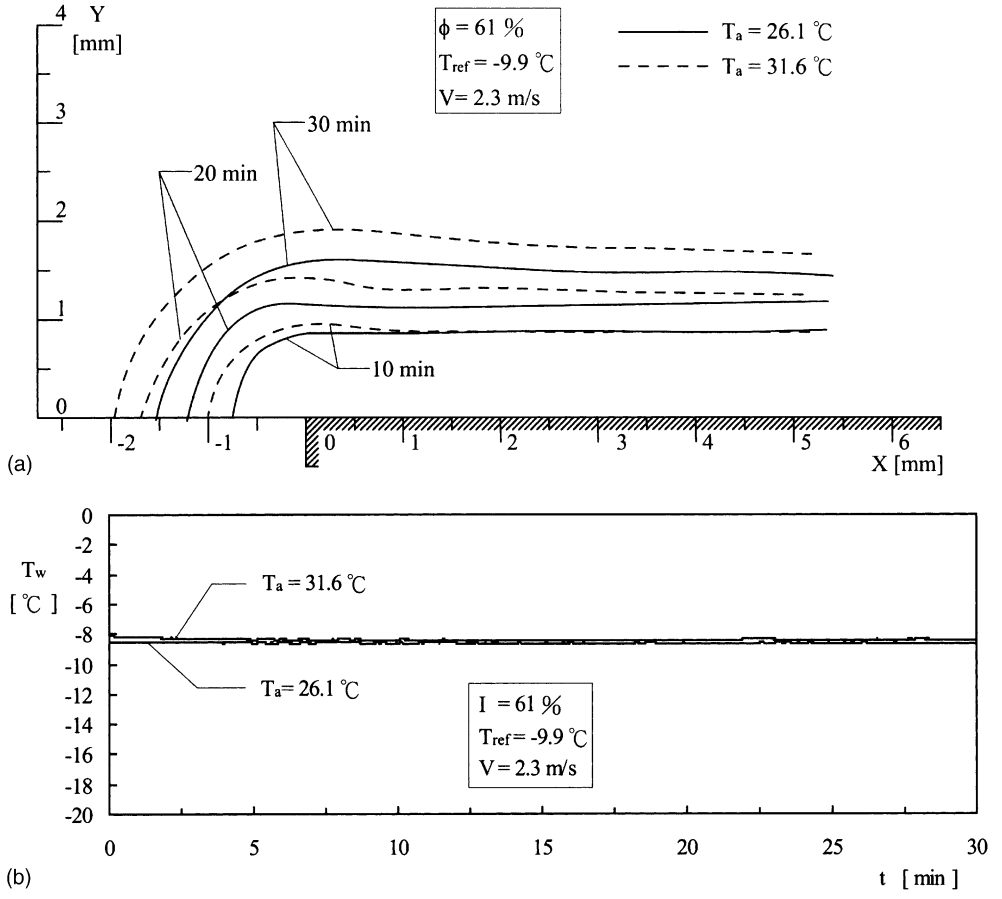

Fig. 9. Effects of air temperature on growth of frost layer adjacent to the leading edge at $\phi = 61\%$, $T_{ref} = -9.9$ °C, and $V = 2.3$ m/s: (a) outlines of the frost layer, (b) histories of cold plate temperature at various air velocities.

nearly coincide with each other with only a very small discrepancy.

Effects of the air temperature on the frost layer adjacent to the leading edge for the case at $\phi = 61\%$, $T_{ref} = -9.9$ °C, and $V = 2.3$ m/s and at $\phi = 64\%$, $T_{ref} = -9.6$ °C, and $V = 5.3$ m/s are shown in Figs. 9 and 10, respectively. For the case with lower air velocity ($V = 2.3$ m/s) considered in Fig. 9, in general the frost thickness increases with the air temperature for the entire frost layer. However, for the case with higher air velocity ($V = 5.3$ m/s), when the air temperature is increased from 21.4 to 31.7 °C, the outline of the frost layer is changed from a round-head profile to a sharp-head profile. Hence, at the leading edge the frost thickness becomes thinner as the air temperature is increased. In addition, a higher air velocity leads to a stronger heat convection on the surface of the cold plate and therefore, the air temperature exerts greater influence on the cold plate. This can be evidenced by a comparison between Figs. 9 and 10(b).

3.2. Frost crystal growth

Next, the downstream region is brought into the focus of the microscopic system. Snapshots of the microscopic growing crystal columns are shown to investigate the crystal structures.

Effects of the air velocity on the frost crystal growth at $\phi = 73\%$, $T_a = 25.0$ °C, and $T_{ref} = -14.7$ °C are illustrated in Fig. 11. Three sets of photographs corresponding to three different air velocities ($V = 0$, 1, and 3 m/s) are provided in Fig. 11(a), (b), and (c), respectively. It is found that at $V = 0$ m/s, small, isolated frost crystals grow in the direction normal to the cold plate in a short period of time. The structure of this growing frost crystal looks like a forest consisting of different kinds of growing trees. From the microscopic point of view, the isolated frost crystals exhibit different shapes and growth rates on the cold plate. Precisely speaking, the structure of the frost crystals seems to be random and unpredictable. When the air velocity is elevated, more frost

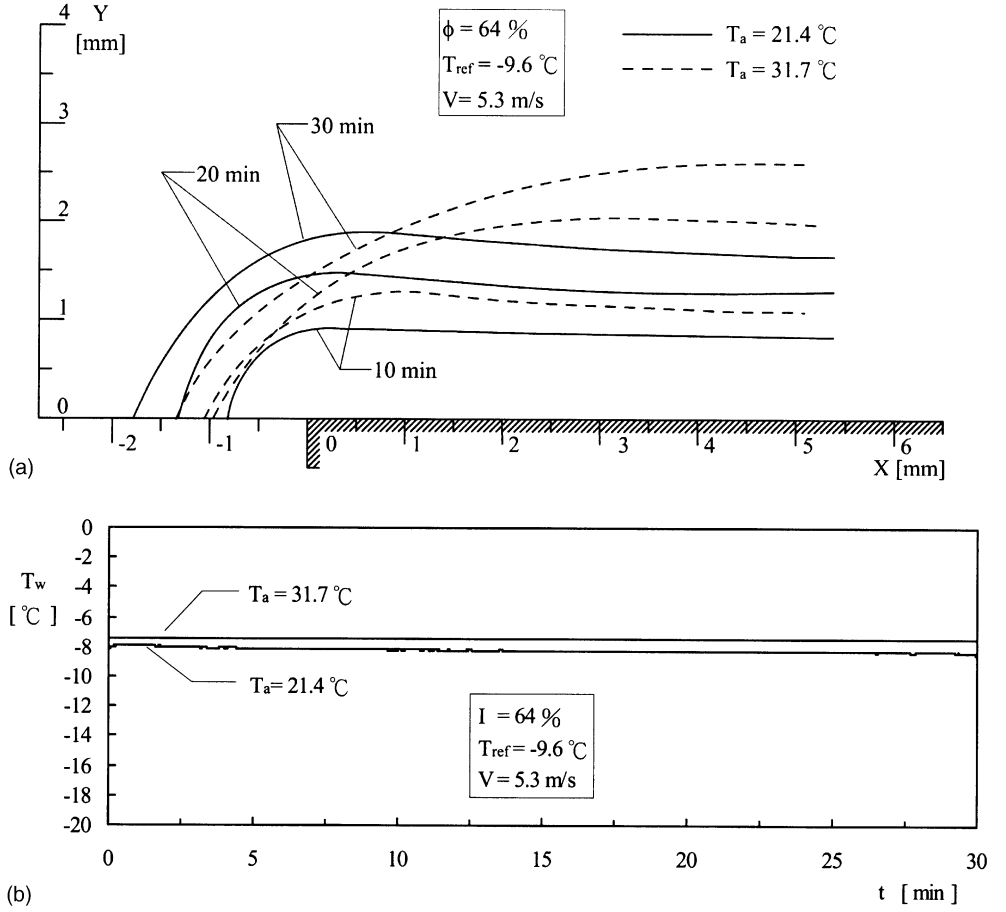

Fig. 10. Effects of air temperature on growth of frost layer adjacent to the leading edge at $\phi = 64\%$, $T_{ref} = -9.6$ °C, and $V = 5.3$ m/s: (a) outlines of the frost layer, (b) histories of cold plate temperature at various air velocities.

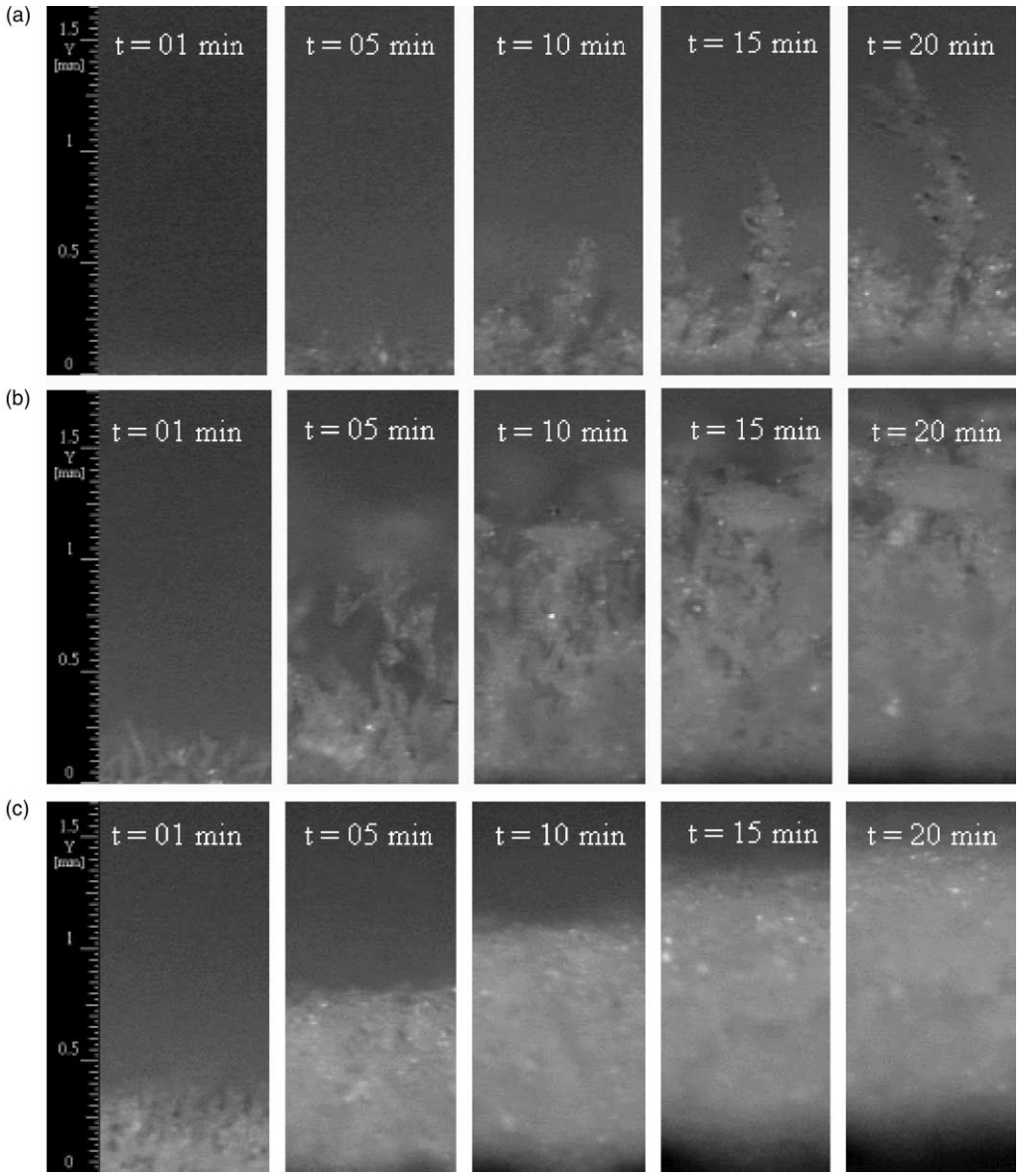

Fig. 11. Effects of air velocity on frost crystal growth at $\phi = 73\%$, $T_a = 25.0$ °C, and $T_{ref} = -14.7$ °C: (a) $V = 0$ m/s, (b) $V = 1$ m/s, (c) $V = 3$ m/s.

crystals are generated. These frost crystals and crystal columns stemming from the existing frost crystal and their branches are formed so that both the thickness and the density of the frost layer increase with time. The density of the frost layer is obviously dependent on the air velocity as shown in Fig. 11.

As stated earlier, both the density and the thickness of the frost layer increase with the relative humidity of the air. Effects of the relative humidity on the pattern of the frost crystals are observed in accordance with the photographs presented in Fig. 12. In this figure, T_a, T_{ref}, and V are fixed at 27.0 °C, −10.2 °C, and 0 m/s, respectively, while ϕ is varied to illustrate the effects of ϕ. These photographs provide direct observation for the dependencies of the frost crystal structure on the relative humidity.

A comparison between Fig. 13(a) and (b) leads to the understanding for the random and unpredictable microscopic features of the frost crystal. Note that the case considered in Fig. 13(a) is maintained at $\phi = 70\%$, $T_a = 25.0$ °C, $T_{ref} = -14.8$ °C, and $V = 0$ m/s, and the case considered in Fig. 13(b) is maintained at $\phi = 70\%$,

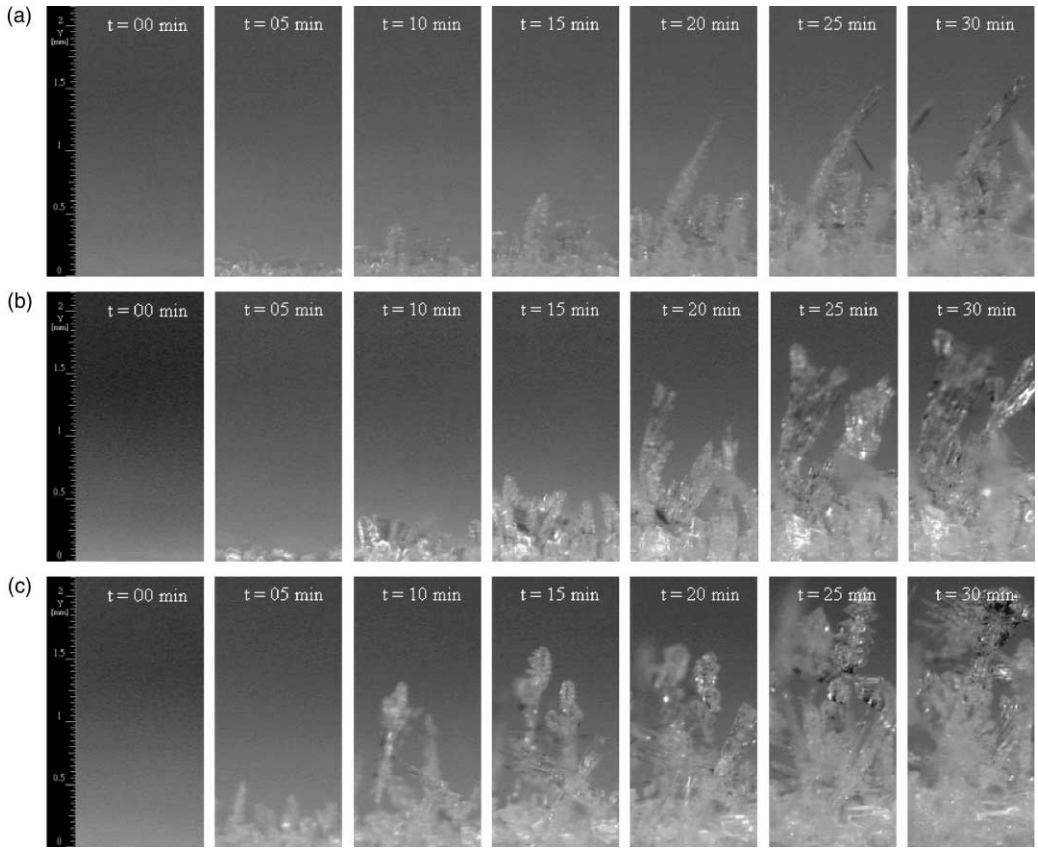

Fig. 12. Growth of frost crystals at $T_a = 27.0$ °C, $T_{ref} = -10.2$ °C, and $V = 0$ m/s: (a) $\phi = 42\%$, (b) $\phi = 48\%$, (c) $\phi = 59\%$.

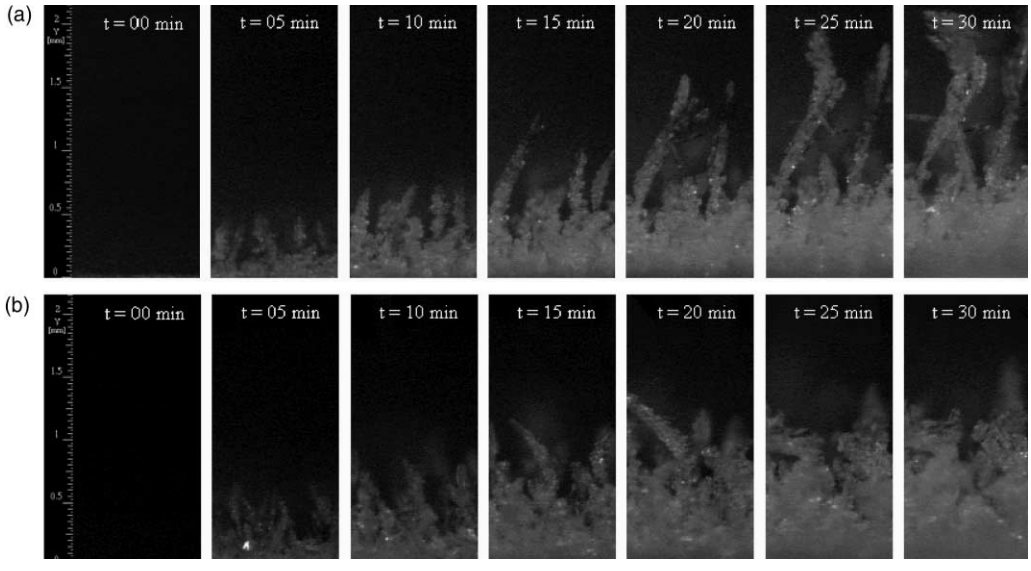

Fig. 13. Growth of frost crystals at $T_a = 25.0$ °C, $\phi = 70\%$ and $V = 0$ m/s: (a) $T_{ref} = -14.8$ °C, (b) $T_{ref} = -16.0$ °C.

$T_a = 25.0$ °C, $T_{ref} = -16.0$ °C, and $V = 0$ m/s. The two sets of environmental variables considered in the two figures are identical except for the cooling refrigerant temperature. However, the photographs shown in the two figures exhibit quite different structures of frost crystals. Based on the observations performed in this study, it seems that the dependence of the frost crystal pattern on the environmental variables is really involved and the frost crystals cannot always be simplified to be simple circular columns in any cases. Therefore, any assumptions for the frost structures must be made carefully in modeling.

4. Concluding remarks

Experimental results regarding the spatial variation of the frost thickness at the leading edge and observation on the growth of the frost crystals are provided. The conclusions reached in this study are summarized as follows:

1. It is found that at the leading edge of the cold plate, the frost crystals grow not only in the direction normal to the cold plate, but also in the direction opposite to the direction of air stream. As a matter of fact, the frost crystals growing in radial direction form a 'round head' at the leading edge. The round head of the frost layer at the leading edge is streamlined by the air flow so that the profile of the round head of the frost layer is rather smooth. In the area adjacent to the leading edge, the thickness of the frost layer is a function of the streamwise location. However, in the downstream region, the frost crystals grow at approximately the same rate, and a homogeneous frost layer of uniform thickness is observed.
2. For the case with lower air velocity, in general the frost thickness increases with the air temperature for the entire frost layer. However, for the case with higher air velocity, the outline of the frost layer is changed from the round-head profile to a sharp-head profile. Furthermore, at the leading edge the frost thickness becomes thinner as the air temperature is increased.
3. At $V = 0$ m/s, small, isolated frost crystals are clearly observed. The structure of the frost layer is like a forest consisting of different kinds of growing trees. From the microscopic point of view, the isolated frost crystals exhibit different shapes and growth rates. The growth of the frost crystals seems to be random and unpredictable. When the air velocity is elevated, more frost crystals are generated. These frost crystals and crystal columns stemming from the existing frost crystal and their branches are formed so that both the thickness and the density of the frost layer increase with time. The dependence of the frost crystal pattern on the environmental variables is really involved and the frost crystals cannot always be simplified to be simple circular columns in any cases. Therefore, any assumptions in modeling for the frost structures must be made carefully.

Acknowledgements

The financial support of this work by National Science Council, Republic of China, under Grant no. NSC 88-2212-E036-003 is gratefully acknowledged.

References

[1] A.F. Emery, B.L. Siegel, Experimental measurements of the effects of frost formation on heat exchanger performance, AIAA/ASME Thermophysics and Heat Transfer Conference, ASME HTD 139 (1990) 1–7.
[2] Y. Hayashi, A. Aoki, S. Adachi, K. Hori, Study of frost properties correlating with frost formation types, J. Heat Transfer 99 (1977) 239–245.
[3] F. Meng, W. Gao, Y. Pan, Growth rate of frost formation through sublimation—a porous medium physical model for frost layer, Proceedings of the 1985 International Symposium, Hemisphere, 1987, 584–593.
[4] P.L.T. Brian, R.C. Reid, Y.T. Shah, Frost deposition on cold surfaces, Ind. Eng. Chem. Fundamentals 9 (1970) 375–380.
[5] B.W. Jones, J.D. Parker, Frost formation with varying environmental parameters, J. Heat Transfer 97 (1975) 255–259.
[6] S.M. Sami, T. Duong, Mass and heat transfer during frost growth, ASHRAE Trans. 95 (1989) 158–165.
[7] S.A. Sherif, R.M. Abdel-Wahed, M.A. Hifni, A mathematical model for the heat and mass transfer on a flat plate under frosting conditions, Proceedings of the 1988 National Heat Transfer Conference, ASME HTD Vol. 96 (1988) 301–306.
[8] Y.X. Tao, R.W. Besant, Y. Mao, Characteristics of frost growth on a flat plate during the early growth period, ASHRAE Trans. 99 (1993) 746–753.
[9] R. Östin, S. Andersson, Frost growth parameters in a forced air stream, Int. J. Heat Mass Transfer 34 (1991) 1009–1017.
[10] A.Z. Şahin, An Experimental Study on the initiation and growth of frost formation on a horizontal plate, Experimental Heat Transfer 7 (1994) 101–119.
[11] D.L. O'Neal, D.R. Tree, Measurement of frost growth and density in a parallel plate geometry, ASHRAE Trans. 90 (1984) 278–290.
[12] D.L. O'Neal, D.R. Tree, A review of frost formation in simple geometries, ASHRAE Trans. 91 (1985) 267–281.
[13] A. Lüer, H. Beer, Frost deposition in a parallel plate channel under laminar flow conditions, Int. J. Therm. Sci. 39 (2000) 85–95.

[14] M.M. Padki, S.A. Sherif, R.M. Nelson, A simple method for modeling the frost formation phenomenon in different geometries, ASHRAE Trans. 95 (1989) 1127–1137.
[15] C.H. Cheng, Y.C. Cheng, Predictions of frost growth on a cold plate in atmospheric air, Int. Comm. Heat Mass Transfer 28 (2001) 953–962.
[16] K.H. Wu, Experimental study of frost formation on a cold plate in humid air flow, M.S. Thesis, Tatung University, Taipei, Taiwan, 2000.
[17] S.J. Kline, F.A. McClintock, Describing uncertainties in single-sample experiments, Mechanical Engineering 75 (1953) 3–8.
[18] R.J. Moffat, Describing the uncertainties in experimental results, Experimental Thermal and Fluid Science 1 (1988) 3–17.
[19] C.H. Cheng, H.N. Chen, W. Aung, Experimental study of the effect of transverse oscillation on convection heat transfer from a circular cylinder, J. Heat Transfer 119 (1997) 474–482.